

# Proteomic Studies of a Single CNS Synapse Type: The Parallel Fiber/Purkinje Cell Synapse

Fekrije Selimi<sup>1,2,3</sup>, Ileana M. Cristea<sup>4,5</sup>, Elizabeth Heller<sup>1</sup>, Brian T. Chait<sup>4</sup>, Nathaniel Heintz<sup>1\*</sup>

**1** Laboratory of Molecular Biology, Howard Hughes Medical Institute, The Rockefeller University, New York, New York, United States of America, **2** CNRS, UMR7102, Paris, France, **3** UPMC, UMR7102, Paris, France, **4** Laboratory for Mass Spectrometry and Gaseous Ion Chemistry, The Rockefeller University, New York, New York, United States of America, **5** Department of Molecular Biology, Princeton University, Princeton, New Jersey, United States of America

**Precise neuronal networks underlie normal brain function and require distinct classes of synaptic connections. Although it has been shown that certain individual proteins can localize to different classes of synapses, the biochemical composition of specific synapse types is not known. Here, we have used a combination of genetically engineered mice, affinity purification, and mass spectrometry to profile proteins at parallel fiber/Purkinje cell synapses. We identify approximately 60 candidate postsynaptic proteins that can be classified into 11 functional categories. Proteins involved in phospholipid metabolism and signaling, such as the protein kinase MRCK $\gamma$ , are major unrecognized components of this synapse type. We demonstrate that MRCK $\gamma$  can modulate maturation of dendritic spines in cultured cortical neurons, and that it is localized specifically to parallel fiber/Purkinje cell synapses in vivo. Our data identify a novel synapse-specific signaling pathway, and provide an approach for detailed investigations of the biochemical complexity of central nervous system synapse types.**

Citation: Selimi F, Cristea IM, Heller E, Chait BT, Heintz N (2009) Proteomic studies of a single CNS synapse type: The parallel fiber/Purkinje cell synapse. *PLoS Biol* 7(4): e1000083. doi:10.1371/journal.pbio.1000083

## Introduction

Each of the thousands of cell types present in the nervous system receives multiple classes of inputs that are spatially segregated and functionally distinct. The chemoaffinity hypothesis stated that “the establishment and maintenance of synaptic associations were conceived to be regulated by highly specific cytochemical affinities...” [1]. Support for this idea has come from studies of specific synaptic proteins [2,3]. For example, different sets of neurotransmitter receptors are found at different synapse types [3], even at excitatory synapses made on the same neuron [4]. Precise subcellular targeting of synapses is also dependent on the recognition of specific molecules such as adhesion proteins [5]. In addition to these direct-recognition mechanisms, guidepost cells seem to target synapse formation to precise locations: their role has been demonstrated in both invertebrates [6] and vertebrates [7]. Synaptic physiology is also regulated by mechanisms that are synapse type-dependent, since similar stimulation patterns can have opposite effects on plasticity of different synapses [8]. Therefore, the formation and function of each type of synapse is controlled by a complex activation of signaling pathways through specific proteins.

Since the visualization of synapses by electron microscopy, attempts have been made at biochemically purifying them and at identifying their chemical composition, especially for the postsynaptic densities characteristic of excitatory synapses [9,10]. The use of mass spectrometry (MS) to identify proteins in complex mixtures has greatly improved our ability to unravel the protein composition of organelles. Using this technique, over 1,000 different postsynaptic proteins have been identified in “bulk” postsynaptic density preparations or in affinity-purified receptor complexes [11–

16]. These proteins have a wide range of functions: receptors to neurotransmitters, scaffold proteins, kinases, enzymes, etc. Recently, combining comparative genomics and proteomics, Emes and collaborators [17] have shown that increased behavioral complexity correlates with a phylogenetic expansion of synaptic proteins that are involved in upstream signaling pathways, such as receptors and adhesion molecules. Microarray analysis also showed a very variable regional expression pattern for these upstream synaptic proteins [17], in accordance with previously obtained results for neurotransmitter receptors [3]. The complexity of the synaptic proteome illustrated by these data highlights the need for studies aimed at systematically identifying the protein composition of individual synapse types, and understanding their mechanistic diversity.

To address this issue, we have developed synaptic protein profiling as an approach to isolate and biochemically characterize specific types of central nervous system (CNS) synapses. We chose to analyze first the parallel fiber to

**Academic Editor:** Huda Y. Zoghbi, Baylor College of Medicine, United States of America

**Received** November 14, 2008; **Accepted** March 2, 2009; **Published** April 14, 2009

**Copyright:** © 2009 Heintz et al. This is an open-access article distributed under the terms of the Creative Commons Attribution License, which permits unrestricted use, distribution, and reproduction in any medium, provided the original author and source are credited.

**Abbreviations:** BAC, bacterial artificial chromosome; CID, collision-induced dissociation; CNS, central nervous system; eGFP, enhanced green fluorescent protein; GFP, green fluorescent protein; MALDI, matrix-assisted laser desorption/ionization; MALDI-IT, matrix-assisted laser desorption/ionization ion trap; MS, mass spectrometry; MS/MS, tandem mass spectrometry; PF/PC synapse, parallel fiber to Purkinje cell synapse; PSD, postsynaptic density; QqTOF, quadrupole/time-of-flight

\* To whom correspondence should be addressed. E-mail: heintz@mail.rockefeller.edu

## Author Summary

The brain is composed of many different types of neurons that form very specific connections: synapses are formed with specific cellular partners and on precise subcellular domains. It has been proposed that different combinations of molecules encode the specificity of neuronal connections, implying the existence of a “molecular synaptic code.” To test this hypothesis, we describe a new experimental strategy that allows systematic identification of the protein composition for individual synapse types. We start with mice that are genetically engineered to facilitate the purification of one type of synapse from a given neuronal population in the central nervous system, the parallel fiber/Purkinje cell synapse. The purification is performed using a combination of biochemical fractionation and affinity purification. Subsequent mass spectrometry allows us to identify approximately 60 different proteins present in the resulting sample. We have further analyzed some of the 60 proteins and show that MRCK $\gamma$ , a newly identified kinase, is localized in the dendritic spines where the parallel fiber/Purkinje cell synapses are formed and that it can modulate the morphogenesis of dendritic spines. The use of this experimental strategy opens up the ability to provide insights into the underlying “molecular code” for the diverse types of synapses in the brain.

Purkinje cell (PF/PC) synapse in the cerebellum, because of its unique physiological properties and its involvement in neurological disease [18,19]. We engineered mice to tag and purify specifically PF/PC synapses and, using MS, we have identified 65 proteins located at the PF/PC synapse. This dataset provides clues to PF/PC synapse-specific signaling pathways, as illustrated by our functional analysis of one of these proteins, MRCK $\gamma$ . Our results provide an important example of the biochemical complexity of an individual synapse type, and reveal a new mechanism for the regulation of synaptic function.

## Results

### Purifying the Parallel Fiber/Purkinje Cell Synapse

To enable purification of PF/PC synapses, we developed a transgenic line that expresses an affinity tag only at the PF/PC synapse. We generated a fusion between the glutamate receptor delta2, GluR $\delta$ 2 (National Center for Biotechnology Information [NCBI]# EDK98768), which is specifically localized at the PF/PC postsynaptic density [20], and Venus, a variant of the green fluorescent protein (GFP). The resulting fusion protein, VGluR $\delta$ 2, is properly processed and transported to the cell surface (Figure S1). To express the fusion specifically in cerebellar Purkinje cells, the VGluR $\delta$ 2 cDNA was then incorporated into a Pcp2 bacterial artificial chromosome (BAC) by homologous recombination, and the resulting Pcp2/VGluR $\delta$ 2 BAC construct was used to generate transgenic mice (Figures 1A and S1). Expression of the fusion polypeptide was detected in the cerebellar extracts of Pcp2/VGluR $\delta$ 2 transgenic mice (Figure 1B), and coimmunoprecipitation experiments demonstrated proper assembly of the VGluR $\delta$ 2 fusion with the endogenous GluR $\delta$ 2 receptor subunits (Figure 1C). As shown in Figure 1D, the localization of VGluR $\delta$ 2 in the molecular layer and somata of PCs agrees with the synaptic localization of the GluR $\delta$ 2 receptor. In contrast, the enhanced GFP (eGFP) control protein expressed using the same BAC vector (Pcp2/eGFP; <http://www.gensat.org>) is detected throughout the cell, including marked

labeling of both Purkinje cell dendrites and axons (Figure 1D). Prior to the affinity-purification step, we sought to produce cerebellar extracts enriched for synaptic structures relative to trafficking complexes, and to maximize the recovery of VGluR $\delta$ 2-tagged postsynaptic densities (PSDs). This was performed by fractionation of a solubilized crude synaptosome fraction (S3) on a gel-filtration column (Figure 2A). As shown in Figure 2B and 2C, this resulted in an enrichment of postsynaptic and mitochondrial proteins, and a relative depletion of endoplasmic reticulum (ER) components and presynaptic proteins in the high molecular weight fractions. These excitatory synaptic fractions contain essentially all of the PSD95 scaffolding protein. They also contain VGluR $\delta$ 2, which was distributed amongst the different fractions in the same manner as wild-type GluR $\delta$ 2 (Figure 2C). This was also observed using a standard synaptosome purification (Figure S2) and shows that the fusion receptor VGluR $\delta$ 2 is targeted to the synapse similarly to the wild-type GluR $\delta$ 2.

To separate PF/PC PSDs from other cerebellar synapses, we performed affinity purification from the pooled excitatory synaptic fractions (red rectangle, Figure 2C) using an anti-eGFP antibody. Electron microscopy of the affinity purified material showed electron-dense structures that were reminiscent of PSDs [21] on the surface of the beads used for purification of VGluR $\delta$ 2 extracts (Figures 3C and S3). These structures were absent from beads used to immunopurify extracts from Pcp2/eGFP control cerebella.

Using western blots, we could show that more than 50% of the target protein was immunopurified from the input extract for either the control eGFP or the VGluR $\delta$ 2 extracts (Figure 3A and unpublished data). Western blotting also demonstrated copurification of several PF/PC synaptic components with VGluR $\delta$ 2, including the GluR $\delta$ 2 and GluR2/3 receptors, and the scaffolding proteins PSD93 and Homer (Figure 3B). Markers of inhibitory synapses (GABA(A) receptor  $\alpha$ 6, GABA(A) receptor  $\beta$ , and gephyrin), presynaptic structures (synapsin I and synaptophysin), or of mitochondria (Cox) did not copurify, demonstrating the specificity of this approach (Figure 3B). As expected, none of these markers copurified with soluble eGFP in extracts prepared from Pcp2/eGFP control mice (Figure 3B). Taken together, these results demonstrate that the combination of cell-specific genetic targeting, molecular tagging of specific CNS synapses, biochemical fractionation, and affinity purification can be used to enrich for a specific type of PSD from crude brain extracts.

### Sixty-Five Proteins Identified in Purified Parallel Fiber/Purkinje Cell Postsynaptic Densities

To systematically identify components of the PF/PC PSDs, we analyzed the protein content of pooled PF/PC PSD preparations using single- and two-stage MS [22]. A first sample, prepared by pooling three experiments using ten Pcp2/VGluR $\delta$ 2 cerebella each, enabled us to identify 12 components present at the PF/PC synapse but not present in the control sample prepared in parallel from Pcp2/eGFP cerebella (Table S1). To increase the number of PF/PC PSD components identified, we performed a second analysis on a sample prepared with a total of 50 cerebella (Figure 3D). A total of 65 proteins were identified: 37 proteins were detected with high confidence (Figures S4 and S5; Tables S1 and S3),

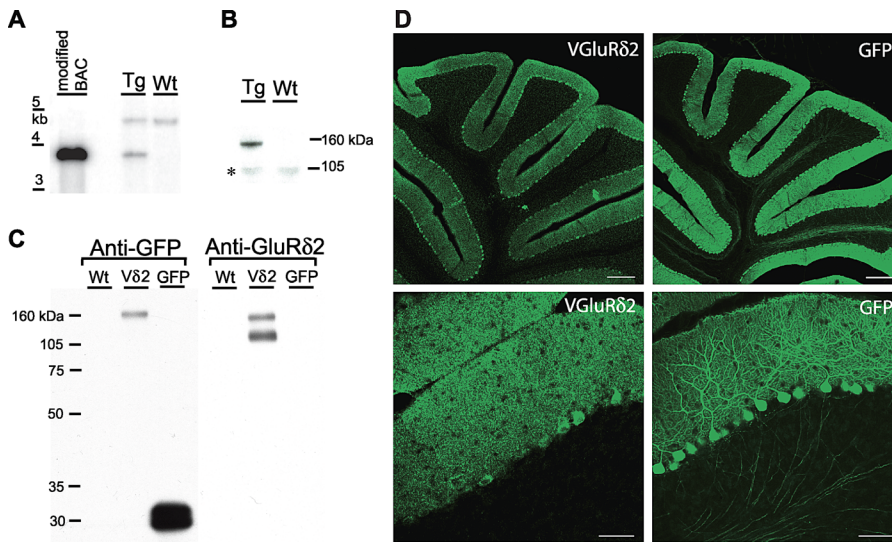


**Figure 1.** Tagging the Parallel Fiber/Purkinje Cell Synapse in Transgenic Mice

(A) Southern blot was used to identify transgenic mice having integrated the *Pcp2* BAC (a Purkinje cell-specific driver) containing the Venus-tagged GluR $\delta$ 2 receptor, VGLuR $\delta$ 2. Tg, transgenic; Wt, wild type.  
 (B) VGLuR $\delta$ 2 expression was detected using an anti-GFP antibody on immunoblots from total protein extracts of transgenic (Tg) versus wild-type (Wt) cerebella. An asterisk (\*) indicates a nonspecific band.  
 (C) Both VGLuR $\delta$ 2 and GFP were affinity purified using an anti-GFP antibody from 1% Triton X-100 cerebellar extracts from wild-type (Wt), *Pcp2*/VGLuR $\delta$ 2 (V $\delta$ 2), and *Pcp2*/eGFP control (GFP) mice, as shown by probing the immunoblots with an anti-GFP antibody (left). VGLuR $\delta$ 2 specifically copurified the endogenous GluR $\delta$ 2, as shown by probing the same blot with an anti-GluR $\delta$ 2 antibody (right).  
 (D) Immunofluorescence on cerebellar sections using an anti-GFP antibody shows the specific localization of VGLuR $\delta$ 2 in the molecular layer and somata of Purkinje cells of *Pcp2*/VGLuR $\delta$ 2 mice. Soluble GFP is detected in the molecular layer, dendrites, somata, and axons of Purkinje cells in sections from *Pcp2*/eGFP mice. Scale bars in the upper panels indicate 200  $\mu$ m; lower panels, 50  $\mu$ m.  
 doi:10.1371/journal.pbio.1000083.g001

and 28 were observed at lower levels and identified with less confidence (Figure S6; Tables S2 and S4). This analysis confirmed the presence of the PF/PC synapse proteins GluR $\delta$ 2 [23], Homer-3 [24], PSD93 [23], delphilin [23], Shank1, and Shank2 [25], and the absence of proteins located at other excitatory (NMDA receptor subunits, GABA(A) receptor  $\alpha$ 6) or inhibitory synapses (GABA(A) receptor  $\alpha$ 6, GABA(A) receptor  $\beta$ , and gephyrin) in the cerebellum. Forty of the identified proteins in our affinity-purified PSDs have been previously detected in preparations of synaptic proteins ([16] and Tables S1 and S2).

The 65 proteins we have identified can be grouped into 11 different functional categories (Figure 3E; Tables S1 and S2). These categories have been previously annotated in studies of the postsynaptic density [13], with the exception of a class of proteins that we have called “phospholipid metabolism and signaling.” In the “scaffolds and adaptors” category, several members of the Shank family (1 and 2) and the PSD family (PSD93 and PSD95) were detected at the PF/PC synapse, illustrating redundancy for scaffold proteins, certainly due to their importance for synaptic function. Other functional categories include proteins important for synapse formation and physiology, such as regulators of small GTPases and protein kinases. Interestingly, eight of the proteins identified in our study can regulate or be regulated by phospholipid metabolism (Iptr1, synaptojanin 1 and 2, phospholipase B, ABCA12, and MRCK $\gamma$ ), or contain phospholipid-binding domains (Plekha7, annexin A6, and MRCK $\gamma$ ), and were thus grouped into a previously unrecognized category “phospholipid metabolism and signaling.” This suggests that phospholipid regulation is a major feature of the PF/PC synapse.

Another important category present at synapses groups receptors and ion channels: several glutamate receptor subunits and several G protein-coupled receptors (GABA-B and BAI receptors) were detected in our analysis of the PF/PC PSD. Interestingly, the extracellular domain of BAI receptors contains thrombospondin repeats, which can mediate cell adhesion [26]. Several other proteins identified at the PF/PC synapse in our study are involved in cell adhesion and interaction with the extracellular matrix: receptor protein tyrosine phosphatases [27], delta-catenin-2 [28], Neph1 [29] and laminins [30]. These diverse potential recognition proteins could form together a “code” defining the PF/PC synapse.

To provide additional evidence for the synaptic localization of the novel components that we have identified, we performed immunofluorescence studies on cerebellar sections from wild-type mice. Localization in the molecular layer of the cerebellum, which contains the PF/PC synapses, was evident for MRCK $\gamma$ , Gm941, BAIAP2, RPTPm, Neph1, and delta2-catenin (Figure 4). Delta2-catenin and Gm941 could also be detected in some cerebellar interneurons. We also examined the expression of candidates reported in in situ hybridization databases (<http://www.stjudebgem.org>; <http://www.brain-map.org>; and <http://www.genepaint.org>). Interpretable data were available for 42 candidates, and all but two were expressed in Purkinje cells, with a majority showing little detectable expression in the granule cell layer (Tables S1 and S2). These expression data provide additional confirmation that the majority of the proteins identified in our study are bona fide components of the PF/PC synapse.



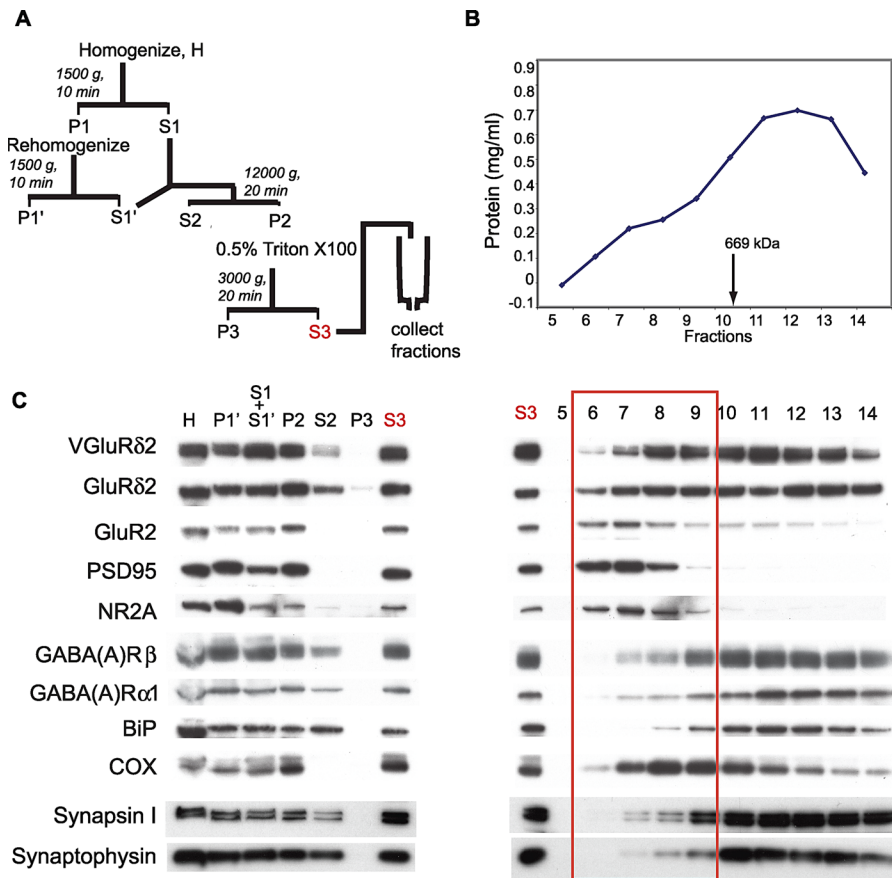


**Figure 2. VGLuR $\delta$ 2 Is Detected in Excitatory Synaptic Fractions Using a New Purification Method**

(A) We prepared a crude synaptosome P2 fraction that was solubilized in 0.5% Triton X-100 final concentration. The extract was then separated on a Sephacryl S1000 gel filtration column. Calibration of the column indicated that protein complexes smaller than 669 kDa (arrow in [B]) were resolved after fraction 10.

(B) Protein dosage was performed on every fraction collected.

(C) Each fraction (0.1% in volume) was run on western blots and assayed for the presence of excitatory postsynaptic markers (GluR $\delta$ 2, GLUR2, PSD95, and NR2A), presynaptic markers (synapsin I and synaptotagmin), inhibitory synapse markers (GABA(A)R $\beta$  and GABA(A)R $\alpha$ 1), the endoplasmic reticulum marker BiP, and the mitochondrial marker COX. VGLuR $\delta$ 2 was detected using an anti-GFP antibody. The red rectangle outlines the “excitatory synaptic” fractions enriched for synaptic markers and pooled for subsequent affinity-purification of PF/PC PSDs.

doi:10.1371/journal.pbio.1000083.g002

### MRCK $\gamma$ : An Example of a New Signaling Pathway at the Parallel Fiber/Purkinje Cell Synapse

Within our “phospholipid metabolism and signaling” category, we identified the kinase MRCK gamma (MRCK $\gamma$ , NCBI# Q80UW5), which has not previously been localized to synapses. Since MRCK family members have been shown to regulate cytoskeleton reorganization and cell morphology [31,32], we sought to test the role of MRCK $\gamma$  in dendritic spine morphogenesis in primary cortical cultures. Comparative analysis of dendritic protrusions was carried out for cultures transfected either with GFP alone, or in combination with full-length MRCK $\gamma$  (MRCK $\gamma$ FL) or a MRCK $\gamma$  construct lacking the kinase domain (MRCK $\gamma$ DN) (Figure 5A). Protrusion density is not significantly affected by overexpression of either form of the kinase (GFP:  $9.5 \pm 0.7$  protrusions per 20  $\mu$ m; MRCK $\gamma$ DN:  $8.0 \pm 0.6$ ; MRCK $\gamma$ FL:  $9.1 \pm 0.6$ ; one-way ANOVA,  $p = 0.29$ ). However, the mean length of dendritic protrusions in neurons overexpressing MRCK $\gamma$ FL decreased when compared to control neurons, whereas the length of protrusions in MRCK $\gamma$ DN-transfected neurons increased

(GFP:  $1.79 \pm 0.07$   $\mu$ m; MRCK $\gamma$ DN:  $2.11 \pm 0.08$ ; MRCK $\gamma$ FL:  $1.48 \pm 0.06$ ;  $p < 0.05$  for all comparisons, Dunn multiple comparison test). The effect of MRCK $\gamma$ DN implies that it can interfere with endogenously expressed MRCK kinases. Indeed, after data mining of previously published results, we found that MRCK $\beta$  has been identified in “bulk” PSD preparations from mouse brain, and thus could be present in cortical neurons [16]. Since mean spine length decreases with maturation [33], our data demonstrate that MRCK family members, through their kinase function, increase maturation of dendritic spines in primary CNS neurons.

Given the presence of MRCK $\gamma$  in our PSD preparations, and its ability to modulate dendritic spine morphogenesis, we were next interested in its subcellular localization in Purkinje cells (Figure 5B). High-resolution confocal immunofluorescence using an antibody against MRCK $\gamma$  clearly demonstrated its presence in Purkinje cell dendritic spines, which have been shown to contain GluR $\delta$ 2 [4]. Moreover, colabeling with markers of specific synapses on Purkinje cells showed that MRCK $\gamma$  is extensively colocalized with VGLuT1, a marker for



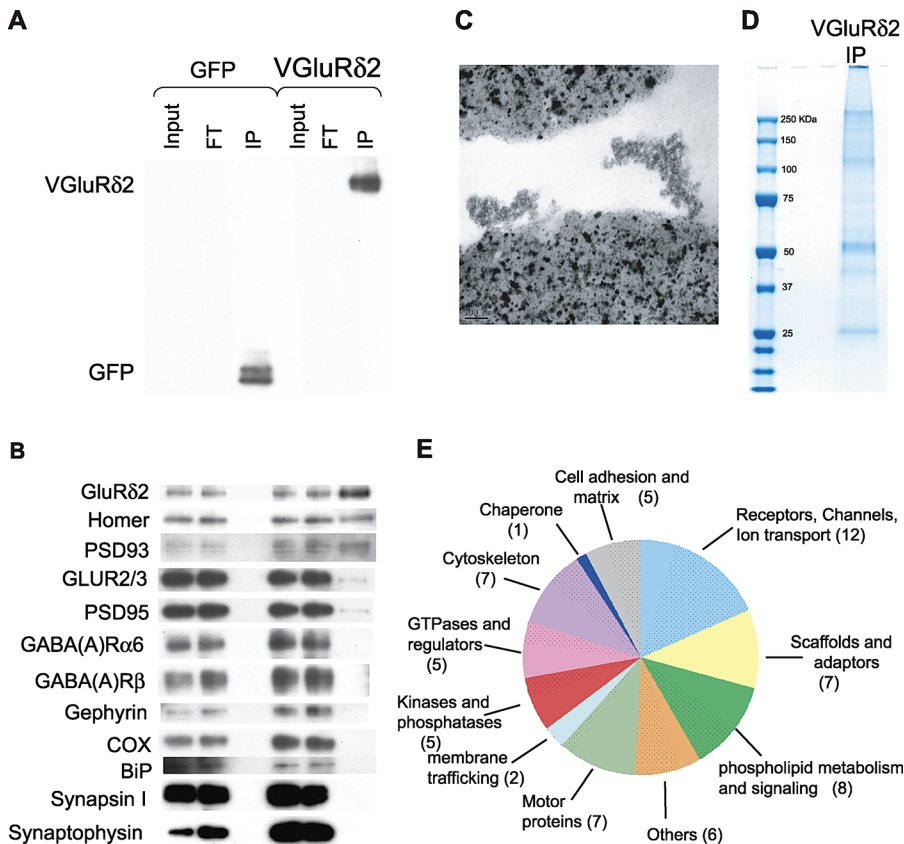


**Figure 3.** Affinity Purification and Protein Profiling of the Parallel Fiber/Purkinje Cell PSDs

(A) Synaptic fractions from Pcp2/VGlur $\delta$ 2 animals were affinity purified using magnetic beads coated with anti-GFP antibody (VGlur $\delta$ 2). In parallel, control purifications were performed on preparations from Pcp2/eGFP transgenic mice (GFP); 0.025% of the inputs and flow-throughs (FT), and 25% of the affinity-purified samples (IP) were assayed by western blot using an anti-GFP antibody and showed immunoprecipitation of both VGlur $\delta$ 2 and GFP, respectively.

(B) The same blot was probed for different postsynaptic markers, presynaptic markers (synapsin I and synaptotagmin), the mitochondrial protein COX, and the ER marker BiP, showing specific copurification of postsynaptic markers localized to the PF/PC synapse.

(C) Electron microscopy shows the presence of electron-dense structures reminiscent of PSDs on the surface of the magnetic beads used for affinity purification of Pcp2/VGlur $\delta$ 2 extracts.

(D) Proteins from the affinity-purified VGlur $\delta$ 2 PSDs were separated by SDS-PAGE electrophoresis and stained with Coomassie Blue before MS analysis.

(E) MS identified 65 different proteins in the complexes purified from Pcp2/VGlur $\delta$ 2 mice. These proteins can be classified into 11 functional categories. The number of proteins from each category is indicated in parentheses. Nonshaded areas represent proteins found with high confidence.

doi:10.1371/journal.pbio.1000083.g003

PF/PC synapses. MRCK $\gamma$  is not present in structures labeled by VGlut2 or GAD65/67, which are present at climbing fiber and inhibitory Purkinje cell synapses, respectively. Taken together, our data support a specific role for MRCK $\gamma$  in the maturation and plasticity of PF/PC synapses, and confirm the importance of synapse-specific protein profiling for the discovery of signaling pathways that modulate the development and function of specific CNS synapse types.

## Discussion

We have demonstrated that the biochemical components of a specific synapse type from a particular neuronal population can be identified using a combination of genetically engineered mice, affinity purification, and MS. Using our approach, we have prepared a fraction enriched in PF/PC PSDs and identified 65 proteins classified in 11 different functional categories. This dataset provides information on signaling pathways specifically tethered to this synapse, as exemplified by our functional analysis of MRCK $\gamma$ .

It also provides information on the variety of proteins that can be part of the code defining the PF/PC synapse.

Approximately 700 different proteins have been identified in PSD preparations from whole brain [16]. However, it has been estimated that, given the mass of a single PSD, the copy number of scaffold proteins in a PSD, and an average size of 100 kDa for each synaptic protein, only about 100 different proteins can be expected to be found at one particular type of PSD [34]. The number of proteins we find in our study is consistent with that estimate. Although our analysis may not have revealed all PF/PC postsynaptic proteins, the successful identification of AMPA receptor subunits in our preparations suggests that any proteins not detected in our sample must be present at low stoichiometries in the PSD.

Synaptic protein profiling can reveal novel sets of proteins that allow formulation of specific hypotheses regarding synaptic function. For example, we discovered MRCK $\gamma$  at PF/PC synapses: this kinase is part of a family that has never been described at synapses. This result was striking since MRCK proteins can respond to small GTPases signaling and

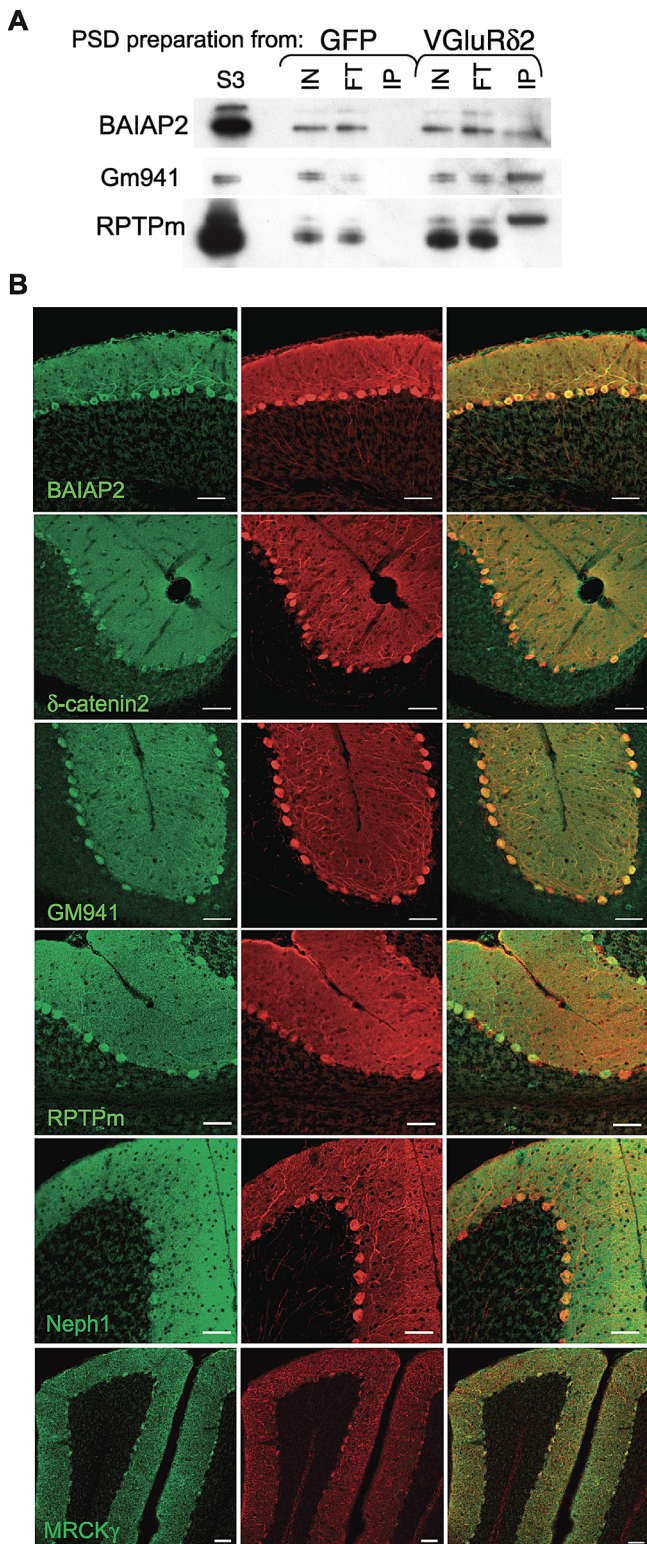


**Figure 4.** Localization of Several Candidate Synaptic Proteins at the Parallel Fiber/Purkinje Cell Synapses

(A) Presence of selected candidates in PF/PC PSDs purified from Pcp2/VGluR $\delta$ 2 cerebella; 0.025% of the inputs (IN) and flow-throughs (FT), and 25% of the affinity-purified samples (IP) obtained from Pcp2/eGFP control (GFP) and Pcp2/VGluR $\delta$ 2 (VGluR $\delta$ 2) cerebella were assayed by western blot.

(B) Localization by immunofluorescence of candidate synaptic proteins. Labeling was performed using antibodies recognizing several candidate proteins identified by MS (green) in conjunction with an anti-calbindin

antibody specifically labeling Purkinje cells (red). Scale bars indicate 50  $\mu$ m.

doi:10.1371/journal.pbio.1000083.g004

have been shown to modulate actin cytoskeleton and cell morphology in nonneuronal systems [31]. These characteristics immediately suggest a role for these kinases in spine morphogenesis, which we have now shown for MRCK $\gamma$  using transfection of cultured cortical neurons. Taken together, these data also have implications for the study of neurodevelopmental diseases. Deficiencies in spine length and spine morphology in Purkinje cells have been found in models of mental retardation and Angelman syndrome [35,36]. Given the link between another small GTPase-dependent kinase, PAK3, and mental retardation [37], our results suggest that MRCK $\gamma$  could participate in the signaling pathways involved in mental retardation and autism spectrum disorders.

Another interesting finding of our study is the presence of a high proportion of proteins involved in phospholipid metabolism and signaling at the PF/PC PSD. A major regulator of the physiology of the PF/PC synapse is the metabotropic glutamate receptor 1 (mGluR1) which induces phosphatidylinositol-4,5-P2 (PIP2) hydrolysis through activation of phospholipase C [8,18]. Our results show the presence of MRCK $\gamma$  and Itp1 in affinity-purified PF/PC PSDs: these proteins can respond to, respectively, DAG and IP3, which are the metabolites of PIP2 hydrolysis. This further supports the importance of mGluR1 signaling at the PF/PC synapse and extends the number of regulatory pathways potentially activated by mGluR1. Also included in the “phospholipid signaling and metabolism” category in our data are synaptojanin-1 and -2, two PIP2-metabolizing enzymes. These enzymes are best known for their regulation of vesicle recycling at synapses, but have also been found by other biochemical studies at PSDs [16]. Phospholipid metabolism is known to be critical for the function of the presynaptic side of the synapse, especially vesicle recycling [38]. It also plays a role in defining the boundaries of the apical pole and the localization of tight junctions in epithelial cells [39]. Our results suggest that phospholipid signaling also participates in regulating the structure and stability of PSDs. Given the fact that lithium is used as a treatment for schizophrenia and bipolar disorders, and that it might act by modulating phospholipids’ metabolism [40], our results may be particularly relevant for studies of a variety of human neurological disorders. Indeed, it has been suggested that synaptojanin-1 is involved in the cognitive defects observed in Down syndrome [41], and that PIP2 metabolism may be linked to synaptic dysfunctions in Alzheimer disease [42].

The results presented here provide clues to the nature of the “synaptic code” and the types of molecules that may be critical in definition of specific synapse types. As expected from previous studies [2], we find proteins with classical adhesion domains such as Neph1 and the receptor tyrosine phosphatase RPTPmu. SYG1, the *Caenorhabditis elegans* homolog of Neph1, has been shown to define synapse location in vivo [6], and may play a similar role for the PF/PC synapse. Receptor tyrosine phosphatases play important roles in axon guidance, and have also been shown to control synapse formation [43]. We also find proteins at the PF/PC synapse with as yet unknown functions in synaptogenesis, such as the



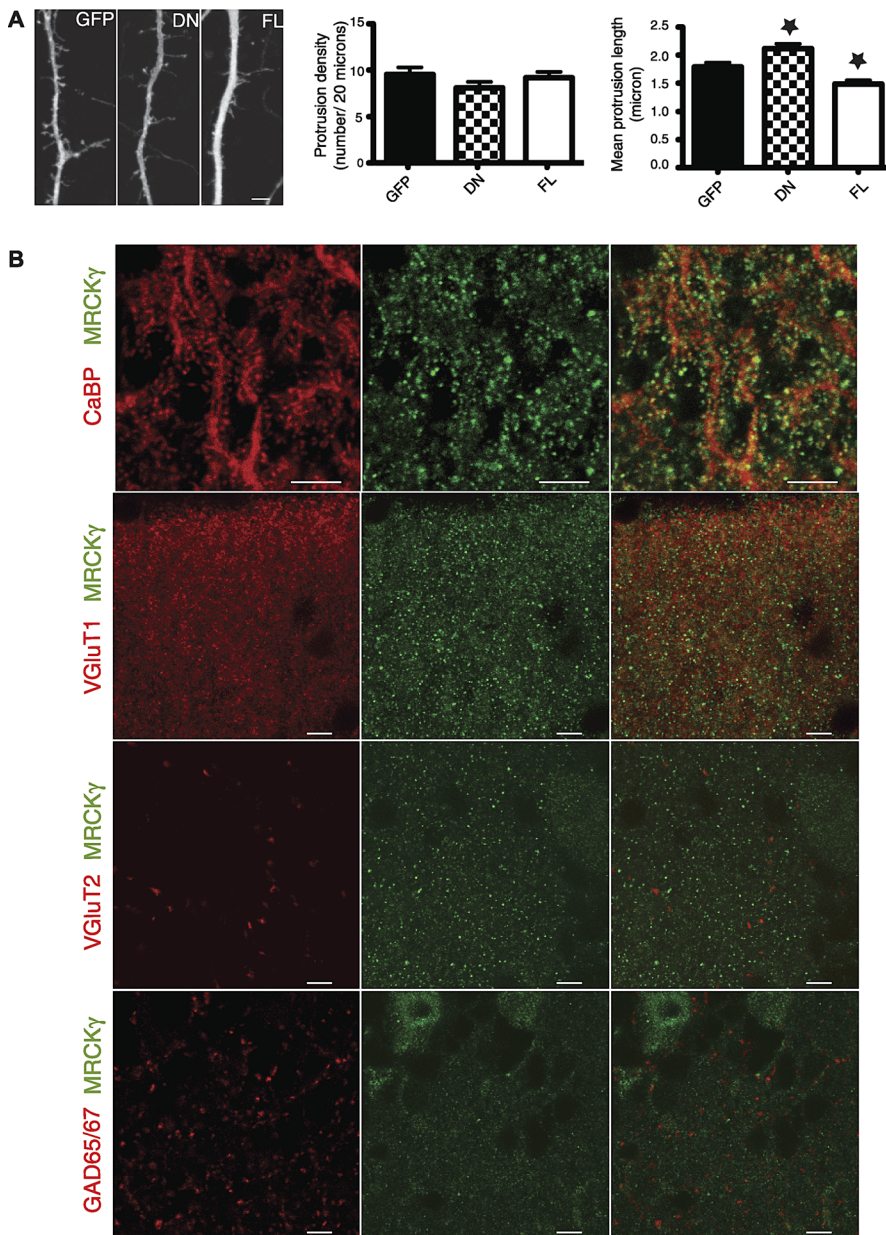


**Figure 5.** MRCK $\gamma$  Modulates Dendritic Spine Morphogenesis and Is Localized to Parallel Fiber/Purkinje Cell Spines

(A) Primary cortical cultures were imaged at DIV14 after transfection with either GFP alone or in conjugation with MRCK $\gamma$  lacking the kinase domain (DN) or the full-length MRCK $\gamma$  kinase (FL) (left panel, scale bar indicates 10  $\mu$ m). Mean protrusion density was not significantly different between the three conditions (middle), but significant changes in mean protrusion length were observed (right panel, asterisk [\*] indicates  $p < 0.05$  compared to GFP).

(B) Immunofluorescence labeling shows the localization of MRCK $\gamma$  (green) in Purkinje cell spines (calbindin, red) and its colocalization with VgluT1, a marker of parallel fiber synapses, but not with VgluT2 or GAD65/67, markers of climbing fiber or of inhibitory synapses respectively. Scale bars indicate 5  $\mu$ m.

doi:10.1371/journal.pbio.1000083.g005

BAI receptors or GABA-B receptors. In this regard, it is interesting to note that the GABA-B receptor 1 contains a CCP module in its extracellular domain. This module is also found in proteins of the complement cascade, which have recently been shown to be involved in synapse development [44]. These proteins, and the majority of the remaining proteins identified in this study, are specifically expressed in Purkinje cells within the cerebellum (see Results). Since cerebellar granule cells also receive excitatory inputs from mossy fibers, we can conclude that, even within the

cerebellum, the synaptic codes for specific synapse types must be quite distinct. This supports the results of expression analysis of proteins identified in bulk synapse preparations showing that receptors and other upstream signaling molecules have a highly variable expression pattern in the vertebrate brain [17]. Taken together, these data indicate that very different sets of molecules must define different excitatory synapse types.

Although our approach employed the expression of a fusion of GluR $\delta$ 2 with EGFP in a specific cell type, this basic



approach can readily be adapted to characterize a wide variety of synapse types, given the wide range of affinity tags that are now available and the hundreds of BAC vectors that can be used to target expression to specific neurons (<http://www.gensat.org>). We anticipate that these additional studies of the biochemical diversity of synapses will be critical for understanding the development and function of specific CNS circuits and their dysfunction in disease [45,46].

## Materials and Methods

**Animals.** All experiments using animals were performed according to protocols approved by the Institutional Animal Care and Use Committee at the Rockefeller University. Both the *Pcp2/eGFP* and the *Pcp2/VGluRδ2* transgenics were bred on the FVB background, and littermates were used as wild-type controls.

**Preparation of PSDs and affinity purification.** Ten cerebella from adult mice were used for the preparation of a crude synaptosome fraction P2 as presented in Figure 2A (based on previously published protocols [47]). The solution used as a homogenization and resuspension buffer contained 0.32 M sucrose, 5 mM HEPES, 0.1 mM EDTA (pH 7.3), and a protease inhibitor cocktail (Sigma). P2 was then solubilized 30 min at 4 °C using a final concentration of 0.5% Triton X-100. The cleared solubilized fraction was separated by gravity flow on a gel-filtration column (Sephacryl S1000 Superfine; GE Healthcare) prepared using a solution containing 2 mM CaCl<sub>2</sub>, 132 mM NaCl, 3 mM KCl, 2 mM MgSO<sub>4</sub>, 1.2 mM NaH<sub>2</sub>PO<sub>4</sub>, 10 mM HEPES, and 0.5% Triton X-100 (pH 7.4). 2-ml fractions were collected, and aliquots were used for protein dosage using the BCA Protein assay kit (Pierce Biotechnology). Calibration of the gel-filtration column was performed using the gel-filtration HMW calibration kit (GE Healthcare).

Pooled fractions from the column were used for affinity purification of tagged PSDs. Dynabeads M-270 epoxy beads (Dyna) were conjugated using 15 μg of affinity-purified goat anti-GFP antibody per milligram of beads [22]; 6 mg of beads were used for affinity purification of pooled synaptic fractions from ten cerebella during 1 h at 4 °C. Beads were then washed in 2 mM CaCl<sub>2</sub>, 300 mM NaCl, 3 mM KCl, 2 mM MgSO<sub>4</sub>, 1.2 mM NaH<sub>2</sub>PO<sub>4</sub>, 10 mM HEPES, and 0.5% Triton X-100. Purified complexes were finally eluted in 0.5 N NH<sub>4</sub>OH, 0.5 mM EDTA for 20 min, dried, and then resuspended in the desired volume of protein electrophoresis sample buffer. Biochemical preparations and affinity purifications were performed in parallel for each genotype, starting with ten cerebella each. For MS analysis, samples from several successive experiments were pooled.

**Mass spectrometry analysis.** Following immunopurification, the isolated proteins were resolved by 1-D SDS-PAGE and stained with Coomassie Blue (GelCode Blue; Pierce). As proteins stain with varied efficiency, for each sample (from the 30- and 50-mice preparations), the complete gel was subjected to mass spectrometric analysis. Each entire gel lane was cut into 66 × 1 mm sections. The 1-mm sections were combined in approximately 30 samples, and proteins were digested with 12.5 ng/μl sequencing-grade modified trypsin (Promega). The resulting peptides were extracted on reverse-phase resin (Poros 20 R2; PerSeptive Biosystems) and eluted with 50% (v/v) methanol, 20% (v/v) acetonitrile, and 0.1% (v/v) trifluoroacetic acid containing 2,5-dihydroxybenzoic acid (2,5-DHB; 1:3 v/v saturated matrix solution in elution solution). Samples were subjected to matrix-assisted laser desorption/ionization (MALDI) quadrupole/time-of-flight (QqTOF) MS and MALDI ion trap (MALDI-IT) tandem MS (MS/MS) analyses using an in-house-built MALDI interface coupled to a Qq-TOF instrument (QqTOF Centaur; Sciex) and an ion trap (LCQDECAXP<sup>PLUS</sup>; Finnigan) as described [22,48,49]. XProteo computer algorithm (<http://www.xproteo.com>) was used to search the peptide fingerprint data and collision-induced dissociation (CID) MS/MS data in the NCBI database (see Text S1). Due to the limited amount of samples, all MALDI-IT CID MS/MS spectra were carefully acquired and interpreted manually. A MS/MS hypothesis-driven approach on isolates from control *Pcp2/eGFP* transgenic mice was used to probe for the specificity of the proteins copurified with VGluRδ2 (Text S1).

**Dendritic spine morphometric analysis.** The MRCKγ cDNA was amplified from cerebellar cDNA. The MRCKγDN construct was obtained by deleting the sequence encoding for amino acids 1–426, and by replacing it with ATG. MRCKγ and eGFP cDNAs were subcloned in the bidirectional Tet-responsive vector pBI (Clontech). Primary neuronal cultures were prepared from E15 mouse

embryos (Swiss strain). Cortices were dissected and triturated using a fire-polished Pasteur pipette and 0.05% trypsin. Neurons were plated on poly-D-lysine and laminin-coated coverslips at a density of  $1.5 \times 10^5$  cells/cm<sup>2</sup> and cultured in neurobasal medium supplemented with 2% B27 supplement, 0.5 mM glutamine, and antibiotics. Transfections were performed at DIV7 with a 1:1 ratio of a tTA-expressing plasmid and the bidirectional vector containing GFP (with or without the kinases) using Lipofectamine 2000 according to the manufacturer's instructions (Invitrogen).

Dendrites of transfected neurons were imaged using a confocal microscope and a 63× objective with a 5× zoom. Quantifications of protrusion density and length were performed using the NeuronJ plugin and the ImageJ software on several dendrites per neuron (at least five different cells per transfection condition, four independent experiments). A total of 1,029, 861, and 950 protrusions were counted and measured for the GFP, DN, and FL transfections, respectively. Statistical analysis was performed using the GraphPad Prism software.

## Supporting Information

**Figure S1.** Construction of a Fusion between Venus and GluRδ2 (VGluRδ2)

(A) Venus was fused on the N-terminal extracellular part of GluRδ2 (top left panel). A GluRδ2-positive band was detected in protein extracts from VGluRδ2-transfected HEK293 cells, but not in extracts from Venus-transfected cells (bottom left panel). The band was at the expected size (about 140 kDa), higher than the endogenous GluRδ2 detected in cerebellar extracts. Immunofluorescence using an anti-GFP antibody detected the extracellular Venus in VGluRδ2-transfected cells in nonpermeabilizing conditions (red, right panels), showing the proper topography of the tagged receptor.

(B) The correct modification of the *Pcp2* BAC with the VGluRδ2 construct was checked by Southern blot (left panel, probe shown in [C]), BAC DNA digested with EcoRI) and pulse-field gel electrophoresis (right panel, BAC DNA digested with SpeI), before injection in mouse oocytes.

(C) Schematic diagram of the BAC containing the *Pcp2* gene, known to be expressed specifically in Purkinje cells. The VGluRδ2 cDNA was placed at the level of the *Pcp2* ATG. The arrow indicates the promoter region.

Found at doi:10.1371/journal.pbio.1000083.sg001 (463 KB AI).

**Figure S2.** VGluRδ2 Is Fractionated Similarly to the Wild-Type GluRδ2 Receptor Using a Classical Synaptosome Preparation

Fractions obtained using the protocol of Dunkley et al. [47] for synaptosome preparation were probed for excitatory synapse markers (GluRδ2, PSD95), the inhibitory synapse marker GABA(A)Rα1, the endoplasmic reticulum marker BiP, and the mitochondrial marker COX. VGluRδ2 was detected using an anti-GFP antibody.

Found at doi:10.1371/journal.pbio.1000083.sg002 (498 KB AI).

**Figure S3.** Immunoelectron Micrograph of Affinity-Purified PSDs from VGluRδ2 Cerebella Labeled with an Anti-PSD95 Antibody

Found at doi:10.1371/journal.pbio.1000083.sg003 (9.05 MB AI).

**Figure S4.** Example of the Mass Spectrometric Strategy Utilized for Protein Identification and Confirmation, Illustrated for PSD93 and PSD95

(A) Following in-gel digestion with trypsin, the mixture of peptides was analyzed by MALDI QqTOF MS. The m/z values of the [M+H]<sup>+</sup> peptides were searched in the NCBI database using the XProteo software, and PSD93 and PSD95 were the first two hits with high scores. The lists of putative peptides generated by the XProteo software are shown, and their presence in the MALDI QqTOF MS is indicated. T, trypsin peptides.

(B) The identity of the proteins was confirmed using MALDI-IT CID MS/MS analyses, and their specificity of isolation was investigated using a hypothesis-driven tandem MS approach on preparations from *Pcp2/eGFP* transgenic mice (GFP). Examples of results from MS/MS analyses on peptides of both high- and low-signal-to-noise ratios are shown.

Found at doi:10.1371/journal.pbio.1000083.sg004 (1.55 MB TIF).

**Figure S5.** The Analysis of Internexin and Camk2b in Immunoaffinity Purifications of VGluRδ2 Exemplifies the Identification and Con-

firmation of Proteins That Were Not Assigned a Score after the Database Search Using the XProteo Software

(A) Internexin and Camk2b peptides were both observed following MALDI QqToF MS analysis; however, only internexin received an XProteo database search score ( $d' = 6$ ).

(B) The presence of both internexin and Camk2b was confirmed using MALDI-IT CID MS/MS analyses.

Found at doi:10.1371/journal.pbio.1000083.sg005 (868 KB TIF).

**Figure S6.** Examples of Spectra Obtained for Low-Confidence Candidates

Representative MALDI-IT CID MS/MS spectra are shown for Atp1a1 and Ncoa7. MALDI QqToF MS data and list of putative peptides are illustrated for Ptpm. The peaks attributed to Ptpm are shown with orange arrowheads. This portion of the gel contained multiple proteins. Light blue and dark blue dots indicate selected peaks attributed to Fodrin alpha chain and traces of GluRδ2, respectively. GluRδ2 was primarily identified in another gel band. Grey dot indicates a heavy labeled GluRδ2 peptide, spiked in all samples containing GluRδ2.

Found at doi:10.1371/journal.pbio.1000083.sg006 (823 KB TIF).

**Table S1.** List of Proteins Identified with Higher Confidence in the Immunisolates of Venus-Tagged GluRδ2

Functional category, expression in Purkinje cells (PCs), and previous identification in PSD preparations (@PSD) are given.

(a) Reference numbers in this column refer to the list in Text S1.

(b) From reference [16]. Y indicates that the protein is detected; N, not detected; and I, the isoform is detected.

Found at doi:10.1371/journal.pbio.1000083.st001 (27 KB XLS).

**Table S2.** List of Proteins Identified in the Immunisolates of Venus-Tagged GluRδ2 with Lower Levels of Confidence as Judged by Mass Spectrometry

Functional category, expression in Purkinje cells (PCs), and previous identification in PSD preparations (@PSD) are given.

(a) Reference numbers in this column refer to the list in Text S1.

(b) From reference [16].

Y indicates that the protein is detected; N, not detected; and I, the isoform is detected.

Found at doi:10.1371/journal.pbio.1000083.st002 (26 KB XLS).

**Table S3.** List of Proteins Identified in the Immunisolates of Venus-Tagged GluRδ2

Results are shown of two replicate experiments from either 30 or 50 mice. The detection and confirmation of the proteins through MS and MS/MS analyses are indicated for both experiments. The sequence coverage, number of peptides, and scores obtained from the analysis of the MALDI QqToF MS spectra are given for the 50-mice experiment. The number and sequences of peptides confirmed by MALDI-IT CID MS/MS analyses are shown for each protein. The presence of these proteins in the control experiment, as judged by hypothesis-driven MS/MS analyses, is indicated. When the presence or absence of the protein could not be judged conclusively, due to either depletion of the sample or inconclusive fragmentation, the entry is marked as not available (n/a). n/o (not observed) in the score column refers to the proteins (MS) or peptides (MS/MS) that were not

## References

- Sperry RW (1963) Chemoaffinity in the orderly growth of nerve fiber patterns and connections. *Proc Natl Acad Sci U S A* 50: 703–710.
- Benson DL, Colman DR, Huntley GW (2001) Molecules, maps and synapse specificity. *Nat Rev Neurosci* 2: 899–909.
- Craig AM, Boudin H (2001) Molecular heterogeneity of central synapses: afferent and target regulation. *Nat Neurosci* 4: 569–578.
- Landsend AS, Amiry-Moghaddam M, Matsubara A, Bergersen L, Usami S, et al. (1997) Differential localization of delta glutamate receptors in the rat cerebellum: coexpression with AMPA receptors in parallel fiber-spine synapses and absence from climbing fiber-spine synapses. *J Neurosci* 17: 834–842.
- Ango F, di Cristo G, Higashiyama H, Bennett V, Wu P, et al. (2004) Ankyrin-based subcellular gradient of neurofascin, an immunoglobulin family protein, directs GABAergic innervation at purkinje axon initial segment. *Cell* 119: 257–272.
- Shen K, Fetter RD, Bargmann CI (2004) Synaptic specificity is generated by the synaptic guidepost protein SYG-2 and its receptor, SYG-1. *Cell* 116: 869–881.

assigned a  $d'$  value from the database search using the XProteo software.

Found at doi:10.1371/journal.pbio.1000083.st003 (57 KB XLS).

**Table S4.** List of Proteins Identified in the Immunisolates of Venus-Tagged GluRδ2 with Lower Levels of Confidence as Judged by Mass Spectrometry

Results are shown from two replicate experiments from either 30 or 50 mice. The detection and confirmation of the proteins through MS and MS/MS analyses is indicated for both experiments. The sequence coverage, number of peptides, and scores obtained from the analysis of the MALDI QqToF MS spectra are given for the 50-mice experiment; a caret (^) indicates a score obtained only after searching manually in the MS spectrum for peptides that could correspond to the protein of interest. The number and sequences of peptides confirmed by MALDI-IT CID MS/MS analyses are shown for each protein. Several proteins were not observed (n/o) at the MS analysis stage, but were identified from MS/MS analyses (not available [n/a]). The presence of these proteins in the control experiment, as judged by hypothesis-driven MS/MS analyses, is indicated. When the presence or absence of the protein could not be judged conclusively, due to either depletion of sample or inconclusive fragmentation, the entry is marked as not available (n/a). n/o (not observed) in the score column refers to the proteins (MS) or peptides (MS/MS) that were not assigned a  $d'$  value from the database search using the XProteo software.

Found at doi:10.1371/journal.pbio.1000083.st004 (28 KB XLS).

**Text S1.** Supplementary Materials and Methods, and Supplementary References

Found at doi:10.1371/journal.pbio.1000083.sd001 (78 KB DOC).

## Acknowledgments

We thank Pr. Cornelia Bargmann and Dr. Anne Schaefer for critical reading of the manuscript and helpful discussions. We also thank the Bioimaging facility at the Rockefeller University, in particular Helen Shio for electron microscopy analysis, and Alison North. We thank Kasia Losos for injection of transgenics, Jie Xing, and Wendy Lee for technical assistance. We thank Dr. Myriam Heiman for help with the goat anti-GFP serum affinity-purification and Pr. Chugh for the anti-Neph1 antibody.

**Author contributions.** FS generated the transgenic mice and performed immunofluorescence studies and functional analysis of MRCKγ. FS and EH performed the biochemical purifications of postsynaptic densities and their western blot analysis. IMC optimized the bead conjugation protocol and performed MS analysis. FS and NH prepared the manuscript. FS, IMC, EH, BTC, and NH discussed the experiments, the data, and the manuscript.

**Funding.** FS was supported by a fellowship from the Human Frontier Science Program Organization, and IMC by The Rockefeller University Women and Science Fellowship CEN5300379. This work was supported by grants from the Simons Foundation and National Institutes of Health grants RR00862 (BTC) and RR02220 (BTC). The funders had no role in study design, data collection and analysis, decision to publish, or preparation of the manuscript.

**Competing interests.** The authors have declared that no competing interests exist.

- Ango F, Wu C, Van der Want JJ, Wu P, Schachner M, et al. (2008) Bergmann glia and the recognition molecule CHL1 organize GABAergic axons and direct innervation of Purkinje cell dendrites. *PLoS Biol* 6: e103. doi:10.1371/journal.pbio.0060103
- Jorntell H, Hansel C (2006) Synaptic memories upside down: bidirectional plasticity at cerebellar parallel fiber-Purkinje cell synapses. *Neuron* 52: 227–238.
- Cotman CW, Banker G, Churchill L, Taylor D (1974) Isolation of postsynaptic densities from rat brain. *J Cell Biol* 63: 441–455.
- Cohen RS, Blomberg F, Berzins K, Siekevitz P (1977) The structure of postsynaptic densities isolated from dog cerebral cortex. I. Overall morphology and protein composition. *J Cell Biol* 74: 181–203.
- Walikonis RS, Jensen ON, Mann M, Provance DW Jr, Mercier JA, et al. (2000) Identification of proteins in the postsynaptic density fraction by mass spectrometry. *J Neurosci* 20: 4069–4080.
- Cho KO, Hunt CA, Kennedy MB (1992) The rat brain postsynaptic density fraction contains a homolog of the Drosophila discs-large tumor suppressor protein. *Neuron* 9: 929–942.
- Peng J, Kim MJ, Cheng D, Duong DM, Gygi SP, et al. (2004) Semi-

- quantitative proteomic analysis of rat forebrain postsynaptic density fractions by mass spectrometry. *J Biol Chem* 279: 21003–21011.
14. Cheng D, Hoogenraad CC, Rush J, Ramm E, Schlager MA, et al. (2006) Relative and absolute quantification of postsynaptic density proteome isolated from rat forebrain and cerebellum. *Mol Cell Proteomics* 5: 1158–1170.
  15. Husi H, Ward MA, Choudhary JS, Blackstock WP, Grant SG (2000) Proteomic analysis of NMDA receptor-adhesion protein signaling complexes. *Nat Neurosci* 3: 661–669.
  16. Collins MO, Husi H, Yu L, Brandon JM, Anderson CN, et al. (2006) Molecular characterization and comparison of the components and multiprotein complexes in the postsynaptic proteome. *J Neurochem* 97 Suppl 1: 16–23.
  17. Emes RD, Pocklington AJ, Anderson CN, Bayes A, Collins MO, et al. (2008) Evolutionary expansion and anatomical specialization of synapse proteome complexity. *Nat Neurosci* 11: 799–806.
  18. Ito M (2001) Cerebellar long-term depression: characterization, signal transduction, and functional roles. *Physiol Rev* 81: 1143–1195.
  19. Polleux F, Lauder JM (2004) Toward a developmental neurobiology of autism. *Ment Retard Dev Disabil Res Rev* 10: 303–317.
  20. Takayama C, Nakagawa S, Watanabe M, Mishina M, Inoue Y (1996) Developmental changes in expression and distribution of the glutamate receptor channel delta 2 subunit according to the Purkinje cell maturation. *Brain Res Dev Brain Res* 92: 147–155.
  21. Vinade L, Chang M, Schlieff ML, Petersen JD, Reese TS, et al. (2003) Affinity purification of PSD-95-containing postsynaptic complexes. *J Neurochem* 87: 1255–1261.
  22. Cristea IM, Williams R, Chait BT, Rout MP (2005) Fluorescent proteins as proteomic probes. *Mol Cell Proteomics* 4: 1933–1941.
  23. Yuzaki M (2003) The delta2 glutamate receptor: 10 years later. *Neurosci Res* 46: 11–22.
  24. Shiraishi Y, Mizutani A, Yuasa S, Mikoshiba K, Furuichi T (2004) Differential expression of Homer family proteins in the developing mouse brain. *J Comp Neurol* 473: 582–599.
  25. Uemura T, Mori H, Mishina M (2004) Direct interaction of GluRdelta2 with Shank scaffold proteins in cerebellar Purkinje cells. *Mol Cell Neurosci* 26: 330–341.
  26. Adams JC, Tucker RP (2000) The thrombospondin type 1 repeat (TSR) superfamily: diverse proteins with related roles in neuronal development. *Dev Dyn* 218: 280–299.
  27. Sallee JL, Wittchen ES, Burridge K (2006) Regulation of cell adhesion by protein-tyrosine phosphatases: II. Cell-cell adhesion. *J Biol Chem* 281: 16189–16192.
  28. Kosik KS, Donahue CP, Israely I, Liu X, Ochiishi T (2005) Delta-catenin at the synaptic-adherens junction. *Trends Cell Biol* 15: 172–178.
  29. Shen K, Bargmann CI (2003) The immunoglobulin superfamily protein SYG-1 determines the location of specific synapses in *C. elegans*. *Cell* 112: 619–630.
  30. Dityatev A, Schachner M (2006) The extracellular matrix and synapses. *Cell Tissue Res* 326: 647–654.
  31. Leung T, Chen XQ, Tan I, Manser E, Lim L (1998) Myotonic dystrophy kinase-related Cdc42-binding kinase acts as a Cdc42 effector in promoting cytoskeletal reorganization. *Mol Cell Biol* 18: 130–140.
  32. Dong JM, Leung T, Manser E, Lim L (2002) Cdc42 antagonizes inductive action of cAMP on cell shape, via effects of the myotonic dystrophy kinase-related Cdc42-binding kinase (MRCK) on myosin light chain phosphorylation. *Eur J Cell Biol* 81: 231–242.
  33. Nimchinsky EA, Sabatini BL, Svoboda K (2002) Structure and function of dendritic spines. *Annu Rev Physiol* 64: 313–353.
  34. Sheng M, Hoogenraad CC (2007) The postsynaptic architecture of excitatory synapses: a more quantitative view. *Annu Rev Biochem* 76: 823–847.
  35. Koekkoek SK, Yamaguchi K, Milojkovic BA, Dordland BR, Ruigrok TJ, et al. (2005) Deletion of FMR1 in Purkinje cells enhances parallel fiber LTD, enlarges spines, and attenuates cerebellar eyelid conditioning in Fragile X syndrome. *Neuron* 47: 339–352.
  36. Dindot SV, Antalffy BA, Bhattacharjee MB, Beaudet AL (2008) The Angelman syndrome ubiquitin ligase localizes to the synapse and nucleus, and maternal deficiency results in abnormal dendritic spine morphology. *Hum Mol Genet* 17: 111–118.
  37. Allen KM, Gleeson JG, Bagrodia S, Partington MW, MacMillan JC, et al. (1998) PAK3 mutation in nonsyndromic X-linked mental retardation. *Nat Genet* 20: 25–30.
  38. Di Paolo G, De Camilli P (2006) Phosphoinositides in cell regulation and membrane dynamics. *Nature* 443: 651–657.
  39. Martin-Belmonte F, Gassama A, Datta A, Yu W, Rescher U, et al. (2007) PTEN-mediated apical segregation of phosphoinositides controls epithelial morphogenesis through Cdc42. *Cell* 128: 383–397.
  40. Halstead JR, Jalink K, Divecha N (2005) An emerging role for PtdIns(4,5)P<sub>2</sub>-mediated signalling in human disease. *Trends Pharmacol Sci* 26: 654–660.
  41. Voronov SV, Frere SG, Giovedi S, Pollina EA, Borel C, et al. (2008) Synaptotagmin 1-linked phosphoinositide dyshomeostasis and cognitive deficits in mouse models of Down's syndrome. *Proc Natl Acad Sci U S A* 105: 9415–9420.
  42. Berman DE, Dall'Armi C, Voronov SV, McIntire LB, Zhang H, et al. (2008) Oligomeric amyloid-beta peptide disrupts phosphatidylinositol-4,5-bisphosphate metabolism. *Nat Neurosci* 11: 547–554.
  43. Dunah AW, Hueske E, Wyszynski M, Hoogenraad CC, Jaworski J, et al. (2005) LAR receptor protein tyrosine phosphatases in the development and maintenance of excitatory synapses. *Nat Neurosci* 8: 458–467.
  44. Stevens B, Allen NJ, Vazquez LE, Howell GR, Christopherson KS, et al. (2007) The classical complement cascade mediates CNS synapse elimination. *Cell* 131: 1164–1178.
  45. Serajee FJ, Nabi R, Zhong H, Mahbulul Huq AH (2003) Association of INPP1, PIK3CG, and TSC2 gene variants with autistic disorder: implications for phosphatidylinositol signalling in autism. *J Med Genet* 40: e119.
  46. Kennedy MB (2000) Signal-processing machines at the postsynaptic density. *Science* 290: 750–754.
  47. Dunkley PR, Heath JW, Harrison SM, Jarvie PE, Glenfield PJ, et al. (1988) A rapid Percoll gradient procedure for isolation of synaptosomes directly from an S1 fraction: homogeneity and morphology of subcellular fractions. *Brain Res* 441: 59–71.
  48. Krutchinsky AN, Kalkum M, Chait BT (2001) Automatic identification of proteins with a MALDI-quadrupole ion trap mass spectrometer. *Anal Chem* 73: 5066–5077.
  49. Krutchinsky AN, Zhang W, Chait BT (2000) Rapidly switchable matrix-assisted laser desorption/ionization and electrospray quadrupole-time-of-flight mass spectrometry for protein identification. *J Am Soc Mass Spectrom* 11: 493–504.